Continental Shelf Research 165 (2018) 26–36

Contents lists available at ScienceDirect

Continental Shelf Research

journal homepage: www.elsevier.com/locate/csr

Intensification of water temperature increase inside the bottom cold water by horizontal heat transport

Xiaojie Yu, Xinyu Guo*

Center for Marine Environmental Study, Ehime University, 2-5 Bunkyo-cho, Matsuyama 790-8577, Japan

ARTICLE INFO

Keywords:
Bottom cold water
Temperature increase range
Horizontal heat transport
Ambient current
Seto Inland Sea
Yellow Sea

ABSTRACT

Bottom cold water (BCW) is widely reported to occur in many coastal areas in summer. Some BCW masses have an increase in temperature of only 1 °C from early spring to summer (e.g., North Sea, Yellow Sea), while the others have a 4–10 °C increase (e.g., Irish Sea, Seto Inland Sea). A model of heat transport with vertical diffusion alone gave good approximation of the temperature increase in the North Sea type BCW masses, while additional heat input from other processes was required to simulate the large temperature increases in Irish Sea type BCWs. BCWs in the Yellow Sea and the Seto Inland Sea are then taken as examples to compare heat transport into the two types of BCWs through three-dimensional numerical modeling. The small warming range of the BCW in the Yellow Sea results mainly from downward heat input by vertical diffusion. In contrast, the large temperature range of warming in the BCW in the Seto Inland Sea is a result of both advection of heat from the surrounding water and vertical diffusion. We therefore infer that advection of heat into the BCW is a necessary condition for the high temperature increase range in Irish Sea type BCWs. Moreover, advection of heat into one BCW in the Seto Inland Sea intensifies from April to July, which is induced by gradually intensified bottom currents. This example supports the importance of heat transport by advection for BCWs where the temporal change in advection of heat is capable of altering the temperature increase rate inside the BCW.

1. Introduction

The presence of bottom cold water (BCW) during summer has been well described in many shelf seas and bays such as the North Sea (James, 1989; Warrach, 1998; Luyten et al., 2003), Yellow Sea (Guan, 1963; Yuan and Li, 1993; Xia et al., 2006), Irish Sea (Horsburgh and Hill, 2003; Holt and Proctor, 2003), and Seto Inland Sea (Guo et al., 2004; Yu et al., 2016). In these coastal regions, the water temperature increase ranges inside the BCW mass differ from spring to summer. For example, in the North Sea, water temperature inside the BCW increases from 7 °C in April to 8 °C in August (Warrach, 1998). In contrast, the water temperature in the BCW in the Irish Sea shows a large increase from 7.5 °C in April to 11.5 °C in August (Holt and Proctor, 2003). Therefore, from the viewpoint of temperature increase range in bottom water masses, the BCWs in the North Sea and Irish Sea show different features: one increases little while the other increases several degrees.

In northwestern Pacific coastal regions, we can also find BCWs with different water temperature increase ranges. The Yellow Sea (Fig. 1) is a semi-enclosed shelf sea connected to the northwestern Pacific through the East China Sea. The tidal current is strong near the coast but weak in the central deep region. In summer, a BCW forms in the central deep basin through weak tidal currents and strong stratification (Guan, 1963; Yuan and Li, 1993; Xia et al., 2006), and the water temperature inside the BCW increases only ~1 °C from spring to summer (Xia et al., 2006). Some recent studies have suggested that the BCW in the Yellow Sea has a southward movement in summer (Zhang et al., 2008; Moon et al., 2009; Wang et al., 2014), and tidal forcing is the dominant factor driving this flow along the western slope while southerly winds and strong surface solar radiation are secondary factors in summer.

The Seto Inland Sea (Fig. 2), a semi-enclosed sea in western Japan, is connected to the Pacific Ocean by the Bungo Channel and Kii Channel and is also impacted by tidal waves entering through these channels (Yanagi and Higuchi, 1981). It consists of many straits and wide basins (called 'nada' in Japanese), and the tidal current is strong in the straits but weak in the wide basins. The presence of BCW mass with different horizontal and vertical scales in summer has been confirmed in several wide basins, including the Iyo-nada (Takeoka et al., 1993; Chang et al., 2009; Yu et al., 2016), Suo-nada (Chang et al., 2009), Hiuchi-nada (Takeoka et al., 1991; Guo et al., 2004; Chang et al., 2009), and Harima-nada (Chang et al., 2009). The temperature increase range in these BCW masses from spring to summer may reach 7–10 °C. Around the BCW, there exists a cyclonic circulation induced by the horizontal

* Corresponding author.
E-mail address: guoxinyu@sci.ehime-u.ac.jp (X. Guo).

https://doi.org/10.1016/j.csr.2018.06.006
Received 7 June 2017; Received in revised form 2 June 2018; Accepted 11 June 2018
Available online 13 June 2018
0278-4343/

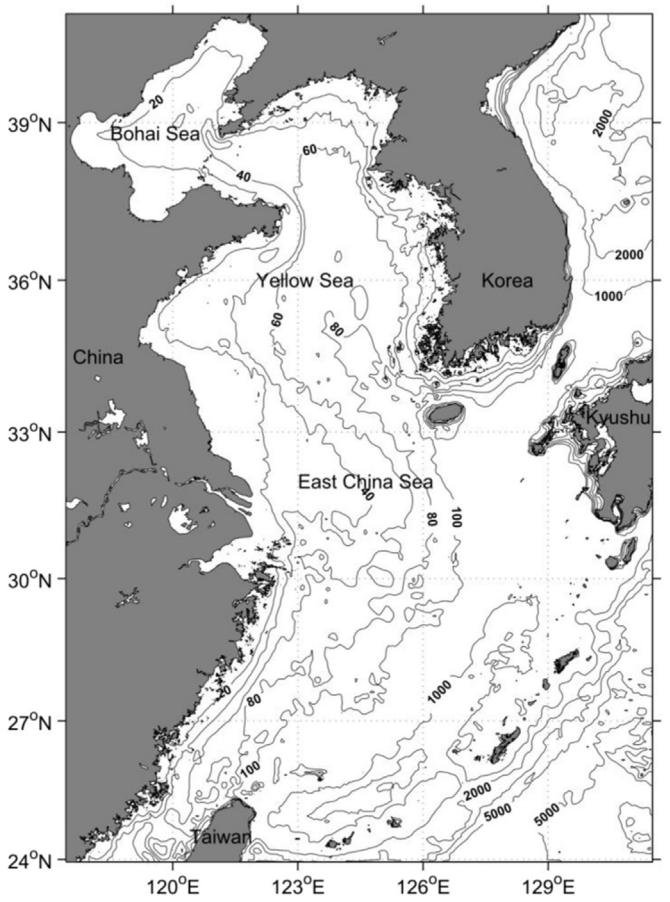

Fig. 1. Bathymetric map showing depth (m) of the Yellow Sea and surrounding water masses and the model domain.

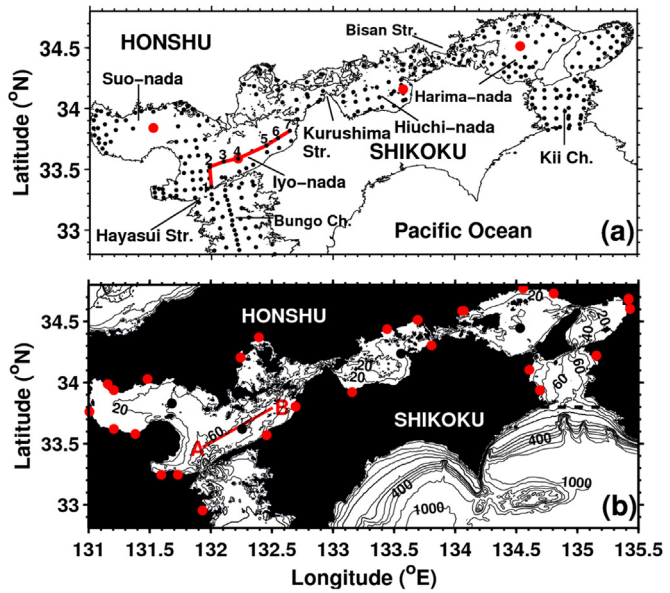

Fig. 2. (a) Monthly sampling stations (black dots) in the Seto Inland Sea. Sampling was conducted at stations 1–7 in Iyo-nada. (b) Bathymetric map showing depth (m) of the Seto Inland Sea and model domain. The open boundaries are the south sides of the Bungo Channel (south boundary) and the Kii Channel (dashed line). The red dots along the coastline denote the mouths of rivers. The red line extending from A to B is the Iyo-nada section. The large red dots in (a) and large black dots in (b) indicate the positions of observed and modeled BCW masses, respectively, in the Iyo-nada, Suo-nada, Hiuchi-nada, and Harima-nada.

gradient of water temperatures across the bottom front of the BCW (Chang et al., 2009; Yu et al., 2016).

Formation of the BCW is generally associated with weak tidal mixing that is not capable of transporting sufficient heat from the surface layer to the bottom layer (He et al., 1959). Therefore, the BCW is usually observed in isolated areas with weak tidal currents and deep water where the Simpson-Hunter parameter ($\log_{10}(H/U^3)$, Simpson and Hunter, 1974) is large, while the surrounding water is relatively warm due to strong tidal mixing that transports heat vertically in the entire water column. However, as we will discuss later, considering only the combination of tidal mixing and water depth, i.e., the Simpson-Hunter parameter, is not sufficient to explain the large increase in water temperature inside the BCW of the Seto Inland Sea. To understand the difference in the water temperature increase range inside the BCW, we take BCWs in the Yellow Sea and the Seto Inland Sea as examples for examining the processes that control heat transport into BCW using numerical modeling. Along with these processes, not only vertical mixing but also water exchange of the BCW with surrounding water is clarified. Such cross-front water exchange has the potential to impact nutrient supply and biological activities (Komorita et al., 2016).

In the next section, we briefly describe the configurations of numerical models used for the Yellow Sea and the Seto Inland Sea, as well as the observation data in the Seto Inland Sea. Section 3 reports the model results for the Yellow Sea and in situ data analysis and model results for the Seto Inland Sea. Section 4 provides interpretation of the differences between BCWs with small and large temperature increases through a comparison of heat transport between the Yellow Sea and the Seto Inland Sea. Section 5 provides a summary of this study.

2. Observation data and model description

2.1. Yellow Sea

To examine BCW and heat transport into the BCW in the Yellow Sea, we adapt a numerical model based on the Princeton Ocean Model (POM, Blumberg and Mellor, 1987; Mellor, 2003). A bathymetric map of the model domain is shown in Fig. 1. The model with a nesting method was set to have a high horizontal resolution (1/18 degrees) for the Yellow Sea and East China Sea and 21 sigma levels in the vertical direction (Guo et al., 2003). Wang et al. (2008) improved the model by including freshwater inputs from the sea surface and rivers and by adding tidal forcing (M_2, S_2, K_1, and O_1 tides) along the lateral boundary. We used the same monthly forcing conditions (heat flux, salt flux, and wind stresses at sea surface; river discharge at river mouths; water temperature, salinity, sub-tidal velocity and elevation at the open boundaries) as Wang et al. (2008) to simulate the stationary seasonal variation in the Yellow Sea and East China Sea. The model was run for 4 years starting from January. We saved the final year model results at 1-h intervals and applied a tide filter given by Hanawa and Mitsudera (1985) to remove tidal signals.

2.2. Seto Inland Sea

The prefectural fishery research centers around the Seto Inland Sea have been carrying out monthly hydrographic observations at 344 hydrographic stations (Fig. 2a) since 1971, providing data on water temperature and salinity at depths of 0, 10, 20, 30, 50, 75, and 100 m from 1971 to 2000. There are four BCW masses in the Seto Inland Sea, one each in the Iyo-nada, Suo-nada, Hiuchi-nada, and Harima-nada (Fig. 4 in Yu et al., 2016). We previously used this data to examine fortnightly variations in the bottom thermal front associated with the BCW in Iyo-nada (Yu et al., 2016). In this study, we chose a station at the center of one BCW in the Seto Inland Sea and fit all water temperature data collected within the BCW over the past 30 years to a curve to examine seasonal variation. By repeating this procedure for all four BCW masses in the Seto Inland Sea (four large red dots in Fig. 2a),

we determined the temperature increase range in the BCW masses from spring to summer.

To examine the heat transport into the BCW masses, we used a numerical model developed for the Seto Inland Sea (Chang et al., 2009). This model is also based on the POM and the bathymetry of the Seto Inland Sea is shown in Fig. 2b. The resolution of the model is ~1 km in the horizontal direction and 21 sigma layers in the vertical direction. This model is driven by monthly heat flux, salt flux, and wind stresses at sea surface; monthly river discharges; and monthly water temperature, salinity, sub-tidal velocity and elevation at open boundary (Chang et al., 2009). Four tidal constituents, M_2, S_2, K_1, and O_1, which have harmonic constants derived from a tide model for larger domains (Guo et al., 2013), are added linearly to the sub-tidal velocity and elevation at the open boundary.

The model calculation was set to start in January and continued for a period of 3 years. Model results were saved hourly, and the impact of tides was removed by the same tide filter used for the Yellow Sea (Hanawa and Mitsudera, 1985). The detided current is termed residual current in this study. The analysis on heat transport into the BCW is based on model results in the third year when the model results nearly coincided with those in the second year.

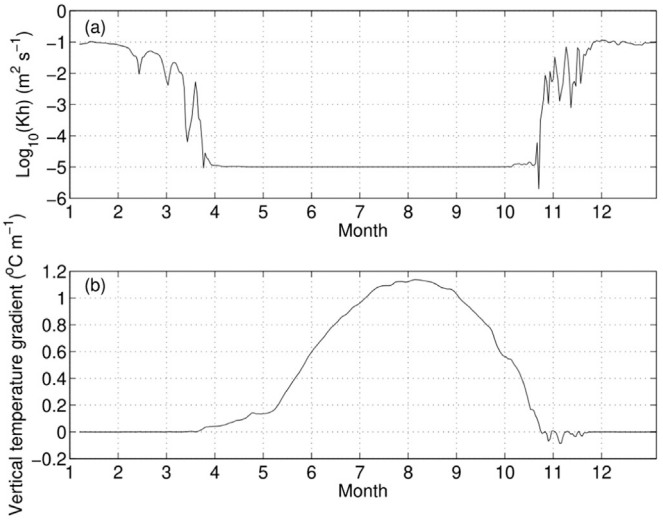

Fig. 4. Time series of vertical diffusivity coefficient ($\log_{10}$ (Kh) $m^2\ s^{-1}$) in the thermocline and the vertical temperature gradient (°C m^{-1}) above the BCW in the Yellow Sea over one year.

3. Results

3.1. Yellow Sea

There are two BCW masses in the Yellow Sea—one in the northern part and the other in the southern part. In this study, we mainly focus on the BCW mass in the South Yellow Sea. Seasonal variation of modeled BCW temperature (black line, Fig. 3a) in the South Yellow Sea showed little increase (~1 °C) from spring to summer, while the surface temperature increase was large (> 20 °C, red line, Fig. 3a). Here, we define spring, summer, autumn and winter in three-month intervals from March to May, June to August, September to November, and December to February, respectively. In summer, the BCW in the South Yellow Sea is centered around 124.5°E, 36.0°N and covers a wide area of approximately 300 km × 300 km. The BCW temperature was only about 6–7 °C, even at the end of July (color, Fig. 3b), which is much lower than the coastal water temperature (~30 °C). The bottom residual current around the BCW is generally weak (arrows, Fig. 3b). The general features of the BCWs in the Yellow Sea reproduced by the model are consistent with the observations (He et al., 1959; Xia et al., 2006; Liu et al., 2009).

In the vertical profile, stratification in the South Yellow Sea was strong in summer, with surface water temperature higher than 25 °C and a bottom water temperature lower than 6 °C (Fig. 3c). The thermocline with strongest stratification was at a depth of 15 m, below which the BCW defined as isothermal lines of 6–7 °C stretches to the sea bottom with a thickness of about 50 m. The BCW forms a bottom front with surrounding water at around 124.0°E and 125.4°E (Fig. 3c).

The time series of the vertical diffusivity coefficient above the BCW at the thermocline (~15 m depth) showed a decreasing trend from winter to spring, remained small (~10^{-5} $m^2\ s^{-1}$) in summer due to strong stratification and then increased to the next winter due to sea surface heat loss and strong winds (Fig. 4a). The background diffusivity coefficient in the model is 10^{-5} $m^2\ s^{-1}$. The vertical temperature gradient above the BCW at ~15 m depth was nearly 0 from winter to spring, gradually increased to ~1.2 °C m^{-1} in summer, and then decreased to 0 in the next winter (Fig. 4b).

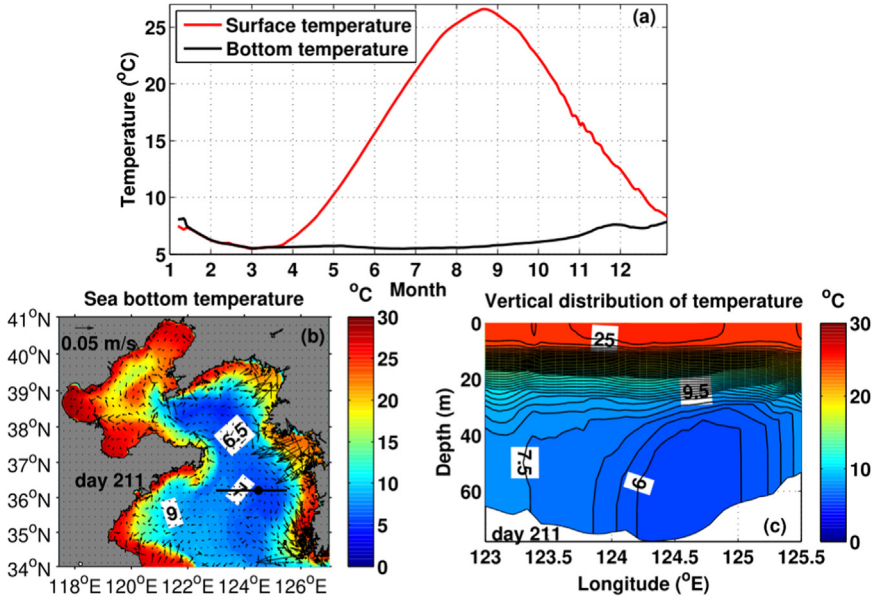

Fig. 3. (a) Model results of seasonal variation in surface and bottom temperatures (°C) at the BCW in the South Yellow Sea at the black dot in (b), (b) horizontal distribution of water temperature (°C, color) and residual current (m s^{-1}, arrows) in the bottom layer on day 211 (31 July), and (c) vertical distribution of temperature (°C) at the section (shown by black line in (b)) on day 211.

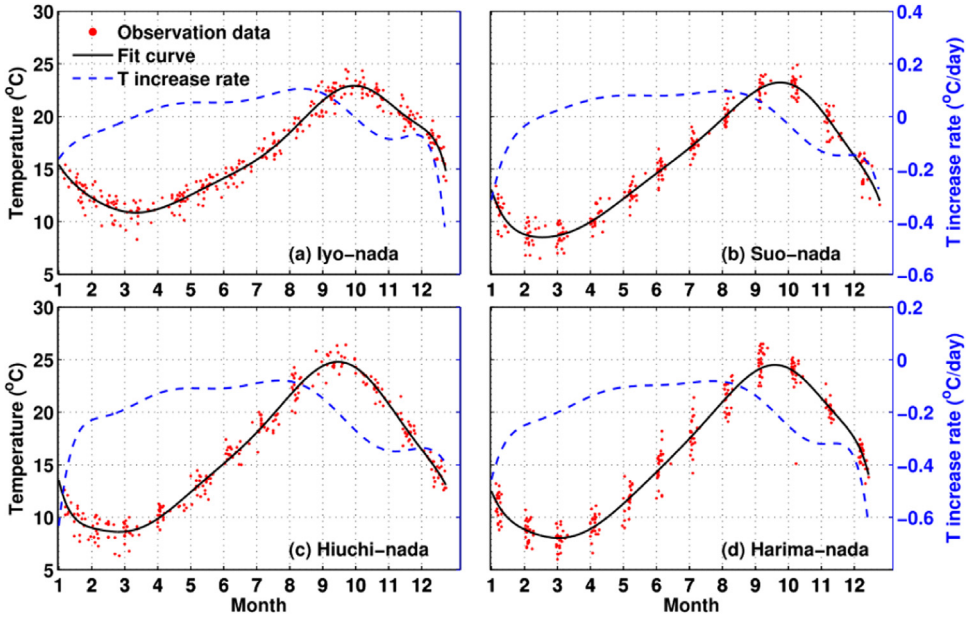

Fig. 5. Observation data (red points), fit curve (black solid lines) of seasonal variation in BCW temperature (°C) and the temperature (T) increase rate (°C/day, blue dashed lines) of the BCW at the points corresponding to red dots in Fig. 2a in (a) Iyo-nada, (b) Suo-nada, (c) Hiuchi-nada, and (d) Harima-nada.

3.2. Seto Inland Sea

3.2.1. Data analysis

Compilation of the monthly minimum temperatures in the four BCW masses in the Seto Inland Sea over 30 years of observations showed clear seasonal variation (black solid lines in Fig. 5, which was obtained by fitting the discrete data to a polynomial function of degree 3 using the least squares method in Matlab). The water temperature range from early April to August was larger in the four BCW masses in the Seto Inland Sea (8–10 °C) than in the Yellow Sea (~1 °C). In addition, the temperature increase rate per day (blue dashed lines, Fig. 5) among the four BCW masses showed differences from early April to August: nearly constant in the Suo-nada (Fig. 5b), Hiuchi-nada (Fig. 5c) and Harima-nada (Fig. 5d), but showing an accelerating trend in the Iyo-nada (Fig. 5a), especially in July.

As an example of warming in the BCW from early spring to summer in the Seto Inland Sea, we show the vertical distribution of temperature, salinity, and density at the section across the BCW in the Iyo-nada (Fig. 6). The temperature of surface water increased from 13 °C in April to 23 °C in July (black lines, Fig. 6), while that of the BCW (lowest depth at Sta. 4) increased from 12 °C in April to 18 °C in July; consequently, stratification above the BCW increased gradually in the nada. Taking the example of the Hayasui Strait (Sta. 1), temperature of the water surrounding the BCW mass was almost uniform throughout the season from the surface to the bottom and was intermediate to that at the surface and bottom of the nada (e.g., Sta. 4). Salinity (color, Fig. 6) showed a decreasing trend over the entire section from April to July. The difference in salinity between the surface and bottom layers in the nada (e.g., Sta. 4) increased, while salinity in the Hayasui Strait (Sta. 1) remained almost uniform over the entire depth. Salinity was always higher in the strait than in the nada. Water density (white lines, Fig. 6) decreased from April to July as a result of increasing water temperature and decreasing salinity. The density difference between the strait and the surface layer of the nada increased from 0.2 kg m^{-3} in April to 1.5 kg m^{-3} in July.

3.2.2. Model results

The modeled water temperature in the BCW masses of the Iyo-nada, Suo-nada, Hiuchi-nada, and Harima-nada all show an increasing trend from spring to summer (black solid lines, Fig. 7). The temperature increase is large from April to August in the nadas (8–10 °C), although the patterns do not exactly match those of the observation data (Fig. 5). Moreover, the temperature increase rate (blue dashed lines, Fig. 7) from spring to summer shows a different pattern in the Iyo-nada (accelerating increase from April to July) (Fig. 7a) compared to those in the Suo-nada (Fig. 7b), Hiuchi-nada (Fig. 7c), and Harima-nada (Fig. 7d) (remaining almost uniform throughout the season).

In the Iyo-nada, the vertical and temporal variation of model results for water temperature (black lines, Fig. 8), salinity (color, Fig. 8), and density (white lines, Fig. 8) show patterns similar to observations (Fig. 6). Moreover, the difference in density between the strait and the surface layer of the nada increased from 0.4 kg m^{-3} in April to 1.8 kg m^{-3} in July. The bottom fronts between the BCW and the surrounding warm water are located about 20–30 km and 50–60 km away from the strait, respectively, and the BCW covers an area with a width of about 40 km and a thickness of 30–40 m on the sea bottom that is defined by the position of isothermal lines arising from the bottom front at 20–30 km.

The vertical diffusivity coefficient in the thermocline (at ~10 m depth) above the BCW in Iyo-nada (Fig. 9a) showed obvious seasonal variation as it was large (10^{-1} m^2 s^{-1}) in winter, decreased sharply from spring to summer (2×10^{-5} m^2 s^{-1}), and increased again from autumn. The background diffusivity coefficient in the model of the Seto Inland Sea was 2×10^{-5} m^2 s^{-1}. A larger background diffusivity coefficient was used for the Seto Inland Sea than for the Yellow Sea because stratification is weaker in the Seto Inland Sea than in the Yellow Sea. The vertical temperature gradient (~10 m depth) above the BCW (Fig. 9b) began to appear in spring, reached a maximum (~0.3 °C m^{-1}) in July, and then decreased again to autumn.

4. Discussion

4.1. Advection of heat from surrounding warm water to the BCW

The BCW in the Yellow Sea has a small temperature increase (~1 °C) from spring to summer, while the BCW masses in the Seto Inland Sea have a large temperature increase of temperature (8–10 °C). Both BCW masses are related to tidal currents that are too weak to generate vertical mixing of the water column in the summer. The question here is whether vertical mixing processes alone can explain the two types of

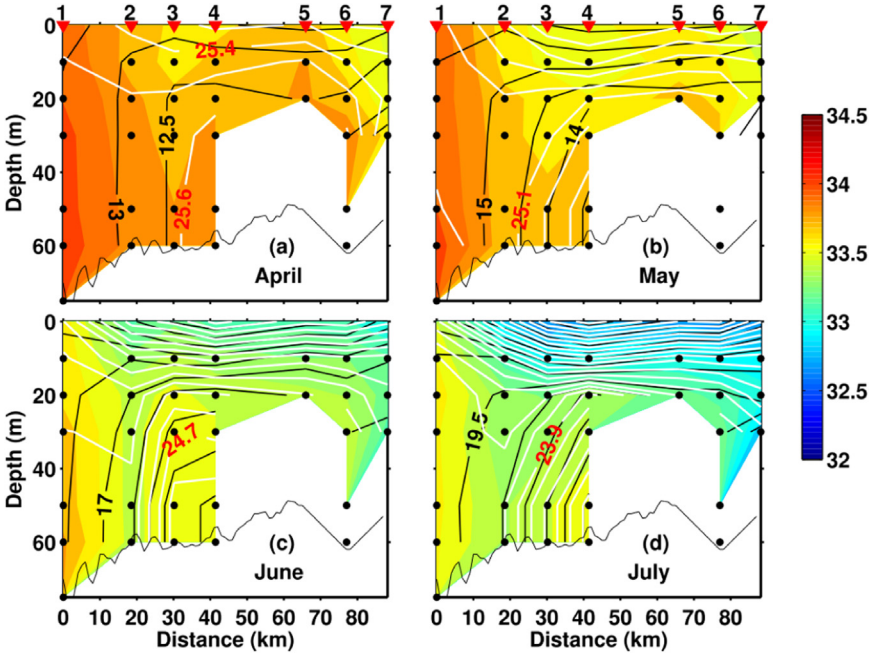

Fig. 6. Vertical distribution of water temperature (°C, black lines), salinity (color), and density (kg m^{-3}, white lines) in Iyo-nada (stations 1–7, Fig. 2a) in (a) April, (b) May, (c) June, and (d) July. Black dots indicate the depth of observation data at each station. Isothermal lines are labeled with black numbers and isopycnal lines are labeled with red numbers.

BCWs. To answer this question, we first examine the capacity of the heat supplied by vertical diffusion into several BCW masses and then quantitatively calculate the contribution of horizontal and vertical processes to the warming of the two types of BCW masses.

4.1.1. Vertical heat transport by diffusion into BCWs

With only vertical diffusion, the water temperature is governed by following equation,

$$\frac{\partial T_v}{\partial t} = \frac{\partial}{\partial z}(K_z \frac{\partial T_v}{\partial z}) \tag{1}$$

where T_v is the water temperature associated with vertical diffusion, and K_z is the vertical diffusivity coefficient. Vertically integrating Eq. (1) from the sea bottom (h_2) to the top of the BCW (h_1) and assuming no heat supply from the sea bottom as well as unchanged thickness of the BCW gives

$$\frac{\partial}{\partial t}\int_{h_2}^{h_1} T_v dz = K_z \frac{\partial T_v}{\partial z}|_{z=h_1} - K_z \frac{\partial T_v}{\partial z}|_{z=h_2} \tag{2}$$

$$\frac{\Delta T_v}{\Delta t}(h_1 - h_2) = K_z \frac{\partial T_v}{\partial z}|_{z=h_1}. \tag{3}$$

From Eq. (3), we can estimate an approximate temperature increase ΔT_v of the BCW over a time period of Δt using vertical diffusivity at the top of the BCW and the vertical gradient of water temperatures across the top of the BCW.

The vertical gradient of water temperature above the BCW is easily derived from observation data. However, the value of K_z is not easily determined. For the Yellow Sea, we used the observed K_z by Liu et al. (2009) of $\sim 10^{-5}$ m^2 s^{-1} near the thermocline in summer, which is

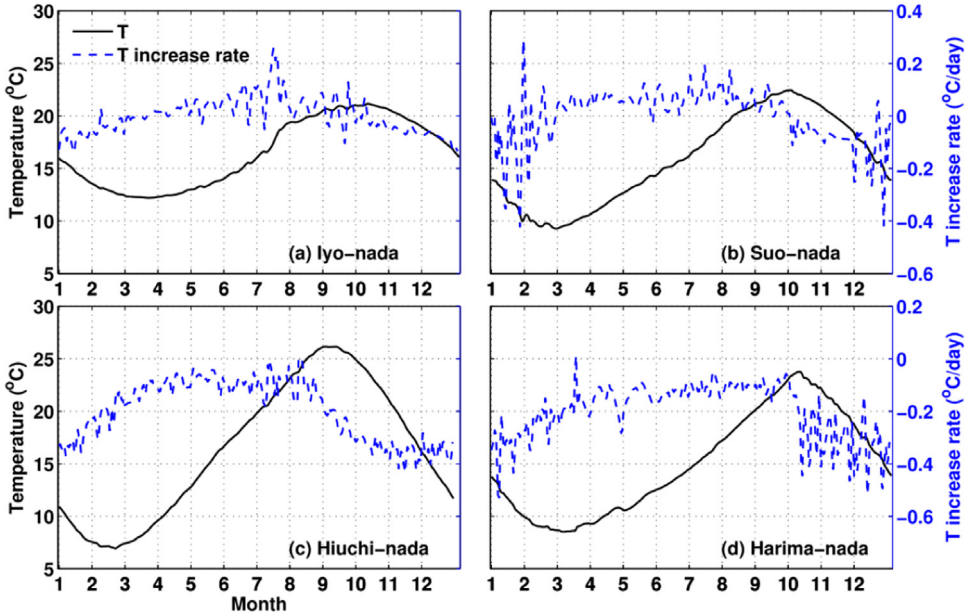

Fig. 7. Model result of seasonal variation in BCW temperature (°C, black solid lines) and the temperature (T) increase rate (°C/day, blue dashed lines) at the points shown by black dots in Fig. 2b in (a) Iyo-nada, (b) Suo-nada, (c) Hiuchi-nada, and (d) Harima-nada.

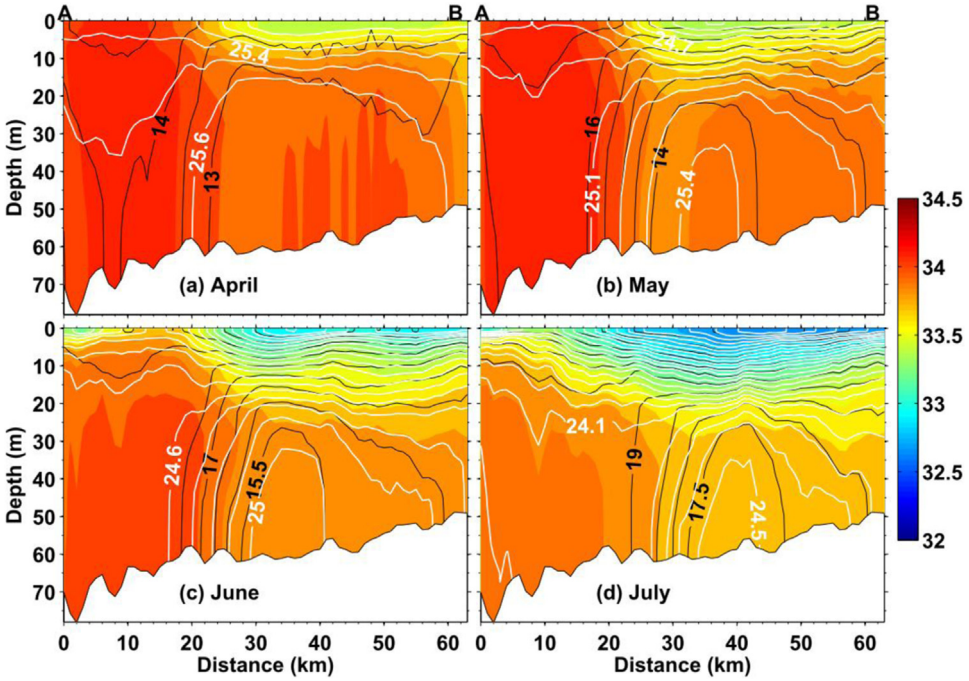

Fig. 8. Vertical distribution of modeled water temperature (°C, black lines), salinity (color), and density (kg m^{-3}, white lines) along section AB in Iyo-nada in (a) April, (b) May, (c) June, and (d) July. Isothermal lines are labeled with black numbers and isopycnal lines are labeled with white numbers.

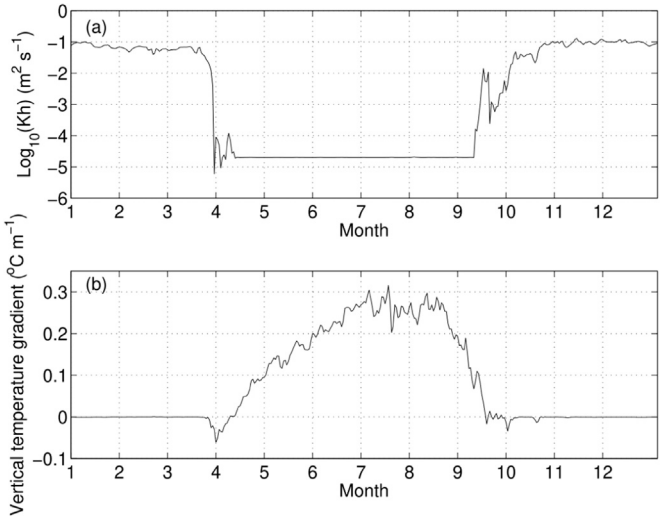

Fig. 9. Time series of vertical diffusivity coefficient ($\log_{10}$ (Kh) m^2 s^{-1}) in the thermocline and the vertical temperature gradient (°C m^{-1}) above the BCW in the Iyo-nada over one year.

consistent with the model result for K_z in our study. Since stratification in the North Sea is as strong as that in the Yellow Sea, we also set K_z to 10^{-5} m^2 s^{-1} in the North Sea. In the Irish Sea, the observation gave an average value of ~6×10^{-5} m^2 s^{-1} near the thermocline (Rippeth et al., 2009). In Iyo-nada, Seto Inland Sea, we used a value of ~2×10^{-5} m^2 s^{-1} generated by our numerical model.

The calculated temperature increase ΔT_v by Eq. (3) and the observed temperature increase ΔT_{real} (Table 1) are consistent for the North Sea and Yellow Sea, which are around 1 °C, indicating that the temperature increase in the BCW there is primarily caused by the vertical diffusion process from spring to summer. In practice, many one-dimensional models have been successfully applied to the North Sea (Sharples and Tett, 1994; Warrach, 1998) and the temperature increase in the BCW has been demonstrated to be mainly due to vertical diffusion of heat.

Table 1
Parameters and calculated ΔT_v and actual temperature increase ΔT_{real} for selected areas. Values for variables are from Warrach (1998) for the North Sea, from Xia et al. (2006) and Liu et al. (2009) for the Yellow Sea, from Holt and Proctor (2003) and Rippeth et al. (2009) for the Irish Sea, and our numerical model for the Iyo-nada of the Seto Inland Sea. The difference in Δt in these seas is due to the different intervals of available water temperature data.

	Δt (d)	$h_1 - h_2$(m)	K_z (m^2 s^{-1})	$\frac{\partial T_v}{\partial z}$ (°C m^{-1})	ΔT_v (°C)	ΔT_{real} (°C)
North Sea	120 6 Apr–4 Aug	40	1.0×10^{-5}	0.35	0.9	1.0
Yellow Sea	90 Apr–Jul	45	1.0×10^{-5}	0.60	1.0	1.0
Irish Sea	100 1 May–10 Aug	60	6.0×10^{-5}	0.2	1.7	4.0
Iyo-nada	120 1 Apr–31Jul.	30	2.0×10^{-5}	0.30	2.1	7.1

Luyten et al. (2003) compared the temperature in the North Sea reproduced with and without an advection term in a three-dimensional model and showed that there was little difference in the temperature of the BCW between two cases, supporting the conclusion that the BCW in the North Sea is not influenced by advection. Wei et al. (2010) demonstrated that interannual variation of temperature in the BCW of Yellow Sea depends primarily on the temperature in the preceding winter, which also indicates that there is little contribution from advective heat transfer to the BCW.

On the other hand, for BCW masses in the Irish Sea and Iyo-nada of the Seto Inland Sea, ΔT_v is much smaller than ΔT_{real} (Table 1). For the Irish Sea, ΔT_v (1.7 °C) is lower than ΔT_{real} (4.0 °C) by 2.3 °C, indicating that heat transfer by other processes must contribute to the warming of the BCW. Horsburgh and Hill (2003) suggested that lateral processes (both diffusion and advection) may be as important as vertical processes in the warming of the BCW in the Irish Sea. Through analysis of the transfer equation for temperature, Holt and Proctor (2003) also concluded that advection of heat from a weakly stratified water mass to the BCW in the Irish Sea is a more important factor than vertical

diffusion of heat. In the Iyo-nada (Table 1), ΔT_v is ~2.1 °C while ΔT_{real} is about 7.1 °C, indicating that other processes of heat transfer can increase the temperature by about 5.0 °C, a contribution that is more than twice that by vertical diffusion from spring to summer.

Therefore, a one-dimensional equation for vertical diffusion is likely capable of reproducing the behavior of BCWs with small temperature increases. However, the BCWs with large temperature increases need more processes to supply heat to the BCW. Apparently, vertical mixing alone is not sufficient to explain the presence of small and large temperature increases in the warming BCWs of shelf seas.

4.1.2. Three-dimensional model analysis of heat transport into the BCWs in the Yellow Sea and Seto Inland Sea

The presence of BCWs is due to a slower increase in water temperature in the sea bottom relative to that of the surrounding water from spring onward. Factors contributing to the heating of the BCW include vertical diffusion of heat from above and advection of and horizontal diffusion of heat from the surrounding warm water. To better understand the processes related to differences between small and large temperature increases in the warming of BCWs, we take the Yellow Sea and Iyo-nada in the Seto Inland Sea as examples and calculate the contribution of each process to the change in water temperature. In the three-dimensional model, the temporal change in water temperature T is controlled by the following equation,

$$\frac{\overline{\partial T}}{\partial t} = \overline{AdvT} + \overline{VdfT} + \overline{HdfT} \tag{4}$$

where $AdvT$ is sum of the advection terms, $VdfT$ is the vertical diffusion term, $HdfT$ is the horizontal diffusion term, and the overbar above each term indicates procedure of detiding. Integrating Eq. (4) over 24 h produces an equation for the daily change in water temperature,

$$\Delta\overline{T}_{daily} = \int_0^{24} \overline{AdvT}\,dt + \int_0^{24} \overline{VdfT}\,dt + \int_0^{24} \overline{HdfT}\,dt. \tag{5}$$

For small temperature increase BCWs, the center of the BCW mass in the South Yellow Sea (black point, Fig. 3b) was chosen to illustrate heat transport into the BCW from April to July (Fig. 10). Temperature variation is relatively large (~0.18 °C day^{-1}) in the surface layer but small (< 0.01 °C day^{-1}) in the bottom layer (Fig. 10a). The sum of the advection terms and the vertical diffusion term (Fig. 10b) show patterns similar to temperature variation (Fig. 10a), indicating that horizontal diffusion of heat plays little role. The advection of heat in the lower layer is very small (Fig. 10c), which means there is little heat supplied from the surrounding warm water to the BCW by advection. Heat input by vertical diffusion is large (~0.18 °C day^{-1}) in the surface layer and small (< 0.01 °C day^{-1}) in the bottom layer (Fig. 10d) due to strong stratification at the depth of 10–20 m (black lines, Fig. 10d). Temperature variation over the entire depth (Fig. 10a) is primarily determined by vertical diffusion of heat (Fig. 10d). As the downward heat by vertical diffusion through the thermocline is limited, the temperature inside the BCW in the South Yellow Sea increases little from April to July.

For large temperature increase BCWs, we chose the center of the BCW mass in the Iyo-nada (black point between A and B, Fig. 2b) to illustrate heat transport into the BCW from early April to the end of July (Fig. 11). The daily increase in water temperature at depths of 20–40 m was small in April (< 0.05 °C day^{-1}) and gradually increased toward July (0.20–0.25 °C day^{-1}, Fig. 11a). The daily change in BCW temperature (T increase rate) is mainly controlled by advection and vertical diffusion since the sum of these terms (Fig. 11b) shows a pattern similar to the daily change in temperature (Fig. 11a). The advection term (Fig. 11c) is always positive in the upper part of the BCW (30–40 m depth) and shows an accelerating trend from April (< 0.05 °C day^{-1}) to July (~0.40 °C day^{-1}) as well as the spring-neap tidal variation. Consequently, advection transfers heat to the area above and to the upper part of the BCW in the Iyo-nada.

A positive (negative) value of the vertical diffusion term indicates that heat is transported downward into the grid is larger (smaller) than that transported downward out of the grid. The vertical diffusion term (Fig. 11d) at the depth of 20 m is very small, indicating that the downward transport of heat by vertical diffusion is limited around the thermocline. However, vertical diffusion is negative (positive) in the upper part (lower part) of the bottom layer, i.e., BCW and also shows an accelerating trend, indicating that vertical diffusion is important to heat redistribution in the BCW.

Apparently, vertical diffusion diffuses heat by advection in the upper part of BCW downward to the lower part of the BCW. Therefore, warming of the entire BCW in the Iyo-nada is under the control of the combination of advection and vertical diffusion. The necessary heat comes mainly from the surrounding warm water with movement of water (advection), and the acceleration of the temperature increase rate in the BCW should be attributed to gradually strengthening advection of heat in the upper part of the BCW from April to July.

To confirm the prevailing effect of advection on the warming of the BCW in Iyo-nada, we carried out another numerical experiment by POM for T_v calculated by Eq. (1) using the same K_z as in Eq. (4) from

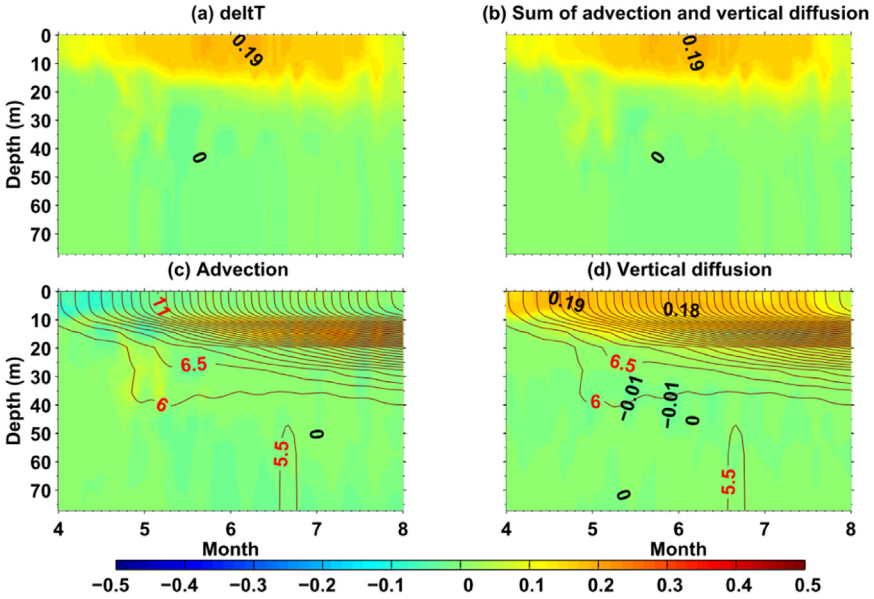

Fig. 10. (a) Daily increase in water temperature (deltT, left hand side of Eq. (5)), (b) sum of advection and vertical diffusion terms on the right hand side of Eq. (5), (c) advection term, and (d) vertical diffusion term. For all panels, T increase rate is shown (color with contour intervals at 0.01 °C day^{-1} with values shown in black from April to July in the BCW (black dot in Fig. 3b) in the South Yellow Sea. Additionally, temperature contours are shown in (c) and (d) by black lines with red labels (°C).

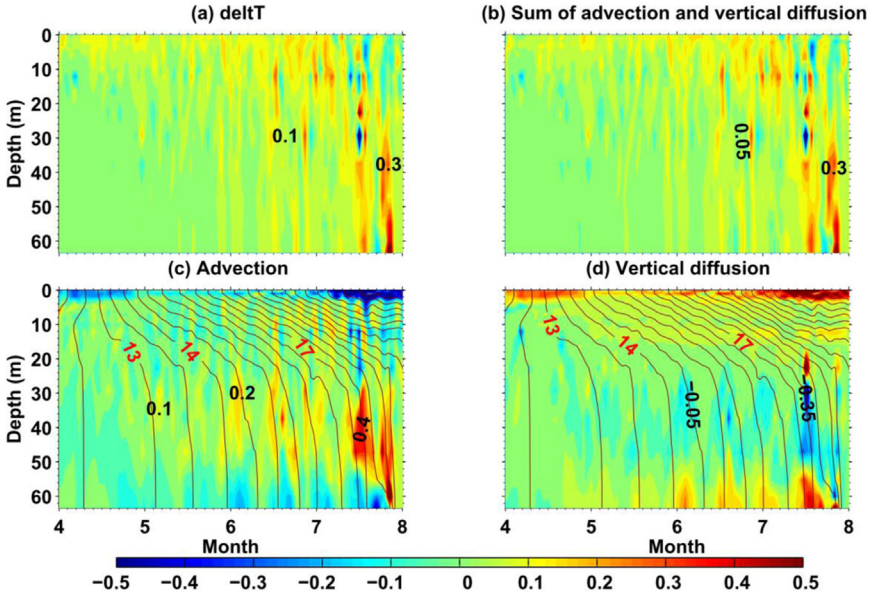

Fig. 11. (a) Daily increase in water temperature (deltT, left hand side of Eq. (5)), (b) sum of advection and vertical diffusion terms on the right hand side of Eq. (5), (c) advection term, and (d) vertical diffusion term. For all panels, T increase rate is shown (color with contour intervals at 0.01 °C day^{-1} with values shown in black from April to July in the BCW (black dot in Fig. 2b) in the Iyo-nada. Additionally, temperature contours are shown in (c) and (d) by black lines with red labels (°C).

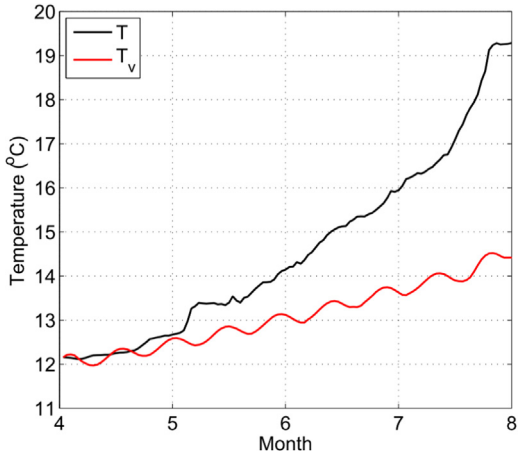

Fig. 12. Time series of bottom water temperature, (°C) in Iyo-nada from April to July. The black line indicates the temperature, T, calculated by Eq. (4) and the red line shows the temperature, T_v, calculated by Eq. (1).

beginning of April when heating becomes positive. The model result at the bottom of Iyo-nada shows that T_v increases from 12.2° to 14.5 °C (2.3 °C) by vertical diffusion alone (red line, Fig. 12), while the temperature T (black line, Fig. 12) increases from 12.2° to 19.2 °C (7.0 °C) by the mechanisms captured in Eq. (4), that is, by advection and vertical diffusion. Vertical diffusion alone can increase the temperature by ~2 °C, being roughly consistent with T_v calculated by Eq. (3), which confirms the rationality of the vertical diffusion equation used in Section 4.1.1. The remaining ~5 °C is increased by the combination of vertical diffusion and advection, confirming again the importance of advection for warming the BCW in the Iyo-nada from spring to summer.

Comparison of heat transport into the BCW masses in the Yellow Sea and in the Seto Inland Sea suggests that small temperature increase in the BCW is mainly due to vertical diffusion of heat, while the large temperature increase BCW is mainly attributable to the combination of advection of and vertical diffusion of heat. Since vertical advection can only redistribute the heat locally, heat transferred horizontally by advection from surrounding warm water should be the cause for the large temperature increase inside the BCW in the Seto Inland Sea.

The importance of heat transfer by advection is heavily location-dependent. We show the horizontal distribution of the percentage of temperature increase controlled by vertical diffusion (percentage of temporal temperature change due to vertical diffusion divided by that due to diffusion and advection) for the BCW, i.e., the temperature change by vertical diffusion from April to July divided by that by diffusion and advection, integrated from the sea bottom to a depth of 20 m (approximately the top of the BCW) in both the Yellow Sea (Fig. 13) and the Seto Inland Sea (Fig. 14). The center of the BCW in the Yellow Sea is mainly warmed by vertical heat diffusion, indicated by a percentage greater than 90%, while the water around the front, especially in the eastern front, is warmed not only by the vertical diffusion with a percentage of about 40%, but also by advection (~60%). In the Seto Inland Sea, the percentage controlled by vertical diffusion is small in Iyo Nada (~40%), but slightly larger in Suo-nada and Harima-nada (~60%). This means that advection of heat is more important to the BCW temperature increase in Iyo Nada (~60%) than in Suo-nada and Harima-nada (~40%).

Therefore, both advection and vertical diffusion occur in heat transport related to the BCW. The small temperature increase BCWs in

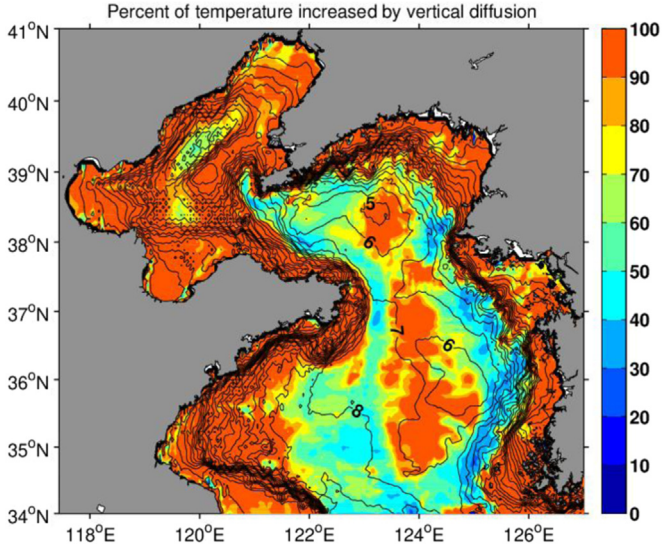

Fig. 13. Horizontal distribution of percentage of temperature increase controlled by vertical diffusion (color) for BCW from the sea bottom to 20 m depth in the Yellow Sea. Black lines indicate the bottom temperature (CI = 1 °C) in July.

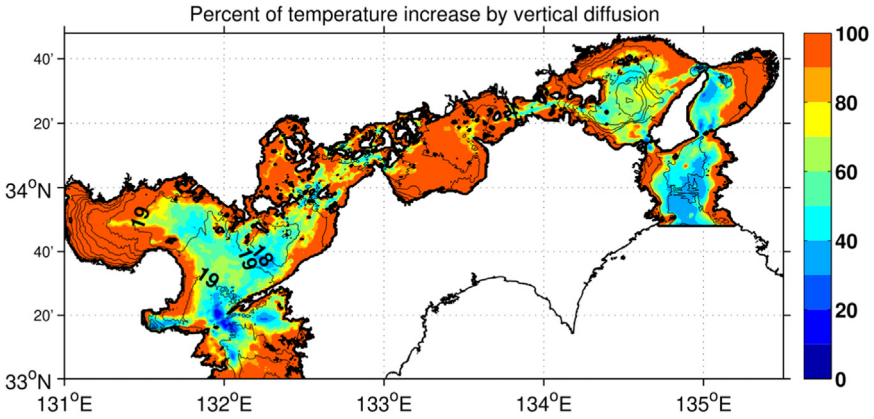

Fig. 14. Horizontal distribution of percentage of temperature increase controlled by vertical diffusion (color) for BCW from the sea bottom to 20 m depth in the Seto Inland Sea. Black lines indicate the bottom temperature (CI = 1 °C) in July.

the literature (Table 1) are located in open, wide regions, such as in the North Sea and Yellow Sea, and have large sizes of about 300 km × 300 km. For these BCW masses, the topography varies smoothly and horizontal currents in the middle and bottom layers are relatively weak. Consequently, advection occurs in the boundary of BCWs while vertical diffusion dominates at the center of the BCWs. On the other hand, the large temperature increase BCW masses are usually located in narrow regions, typically having a small size such as about 100 km × 100 km as in the Irish Sea, and 40 km × 30 km in the Iyo-nada, Seto Inland Sea. In these areas, the topography changes sharply and the horizontal currents in the middle and bottom layers are relatively strong, which can bring heat to the BCW from the surrounding warmer water. In these BCWs, the contribution of advection to warming the BCW differs from each other. In some regions (e.g., the Irish Sea), advection of heat (2.3 °C) plays almost the same role as vertical diffusion of heat (1.7 °C) to BCW warming. In other regions (e.g., Iyo-nada), the contribution of advection (5.0 °C) is more than twice that of the vertical diffusion (2.1 °C) to BCW warming (Table 1).

One problem with our estimation of vertical diffusion is the use of monthly mean forcing in the model calculation. Consideration of short-term variations (e.g., diurnal variation) in winds can introduce more kinetic energy to the ocean than the monthly mean winds and therefore enhance vertical mixing in the surface layer (Lee and Liu, 2005; Cardona and Bracco, 2012). Yu et al. (2017) reported that inclusion of diurnal variation in winds into the model can increase the water temperature inside the BCW of Yellow Sea by 0.4 degrees. Our new calculation for the Seto Inland Sea using hourly winds also shows an increase in the water temperature of the BCW in the Iyo-nada by 1 °C. This process is excluded in both models for the study areas, and while its influences on vertical mixing may partly affect the vertical distribution of calculated water temperature, omitting it may not change our conclusions on the importance of the role of horizontal advection to heat transport into the BCWs in the Seto Inland Sea.

4.2. Model analysis of acceleration of temperature increase rate for the BCW in the Iyo-nada

The BCW in the Iyo-nada has a large temperature increase from spring to summer that is attributed to advective heat transfer from the surrounding warm water. Besides, the temperature increase rate of the BCW accelerates from April to July, which is likely induced by the gradually intensifying advection of heat into the BCW. To examine the specific route of heat transport by advection and its strengthening process, we show the horizontal distribution of the advection term for water temperature in Eq. (5) at a depth of 40 m from April to July (color, Fig. 15). To avoid the influence of spring and neap tides, we selected the days corresponding to spring tide in each month, i.e., days 111, 140, 168, and 196. Positive advection terms between the BCW and Hayasui Strait show an increasing trend and also transition toward the BCW from April to July, and the maximum value always coincides with the temperature front (black lines, Fig. 15).

The advection term is comprised of horizontal and vertical components. Our analysis shows that the horizontal advection brings heat to the upper part of the BCW, while the vertical advection carries water at the upper part of BCW upward to upper layer and downward to bottom layer (figure not shown). This situation is consistent with the hypothesis proposed by Takeoka (2002). Since the horizontal advection of heat is always larger than the vertical advection of heat, the advection ultimately results in a positive value in the upper part of BCW. Moreover, both horizontal and vertical advection terms of heat show accelerating trends from April to July.

We further decomposed the current and temperature data into subtidal component and intra-tidal components and calculate the advection term again. The result shows that advection due to currents and water temperature components with a period shorter than tidal periods is much smaller than that due to currents and water temperature components with a period longer than the tidal period. Therefore, the horizontal advection term of heat is associated with the residual current and temperature gradient.

Since the temperature gradient around the BCW does not change markedly through the season (inferred from the black lines in Fig. 15), the variation in the horizontal advection term of heat is mainly attributed to the residual current, which flows against the temperature gradient direction. From the horizontal distribution of residual current (arrows, Fig. 15) along the 40 m depth, we can see that in April, there is a residual current from the Hayasui Strait to the Iyo-nada, which is limited around the strait. From May to July, the current gradually moves inward toward the nada. When the current flows against the temperature gradient direction, it transports warm water from outside to the inside of BCW, which can explain the coincident positions of the maximum advection term of heat and the temperature front. Therefore, this residual current from the Hayasui Strait to the Iyo-nada in the upper part of the BCW brings heat from warm water to the BCW area and increases the temperature of the BCW through a combination of vertical diffusion and vertical advection inside the BCW. In moving toward the BCW over time, it induces the acceleration of the temperature increase rate of the BCW in Iyo-nada.

To elucidate the physics of this residual current, we examined the vertical distribution of the residual current along the section AB (arrows, Fig. 16). In April, there is an apparent current from the strait to nada, which is actually the tide-induced residual current that is stronger in the surface layer than in the bottom layer. From May to July, the current in the surface layer gradually decreases and reverses direction from nada to strait, while the current in the bottom moves farther to the

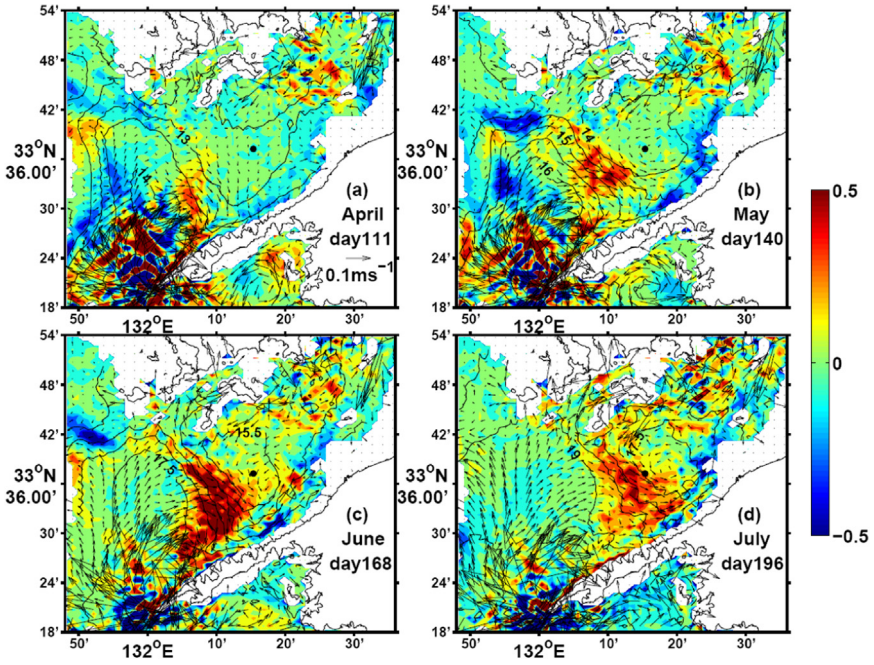

Fig. 15. Horizontal distribution of the advection term for water temperature (°C day^{-1}, color), residual current (m s^{-1}, arrows), and water temperature (°C, black lines) at a depth of 40 m in Iyo-nada in (a) April, (b) May, (c) June, and (d) July.

nada. Taking the actual situation of the Seto Inland Sea into account, we suggest that this current from May to July is a density-induced gravitational circulation. Since the river discharge gradually increases in summer, more low salinity water flows from the east side into the Iyo-nada in the surface layer while saline water from ocean side flows through the Bungo Channel to the Hayasui Strait in the bottom layer. Meanwhile, the temperature in the surface of the Iyo-nada is higher than that in the Hayasui Strait due to strong thermal stratification in the nada. As stated in the model results, owing to the coupled effects of the thermal and saline differences, the density difference between surfaces of the Iyo-nada and the Hayasui Strait increasing from 0.4 kg m^{-3} in April to 1.8 kg m^{-3} in July (Fig. 8) led to the occurrence of gravitational circulation with the surface flow being outward and the bottom flow inward. According to Wong (1994), the velocity of density-induced gravitational circulation is positively correlated with the horizontal density gradient and negatively correlated with the vertical eddy viscosity A_z. The vertical eddy viscosity in the Iyo-nada (color, Fig. 16) decreases from April to July due to stronger stratification. Therefore, with the former increasing and the latter decreasing, the gravitational circulation intensifies from April to July, which finally induces the

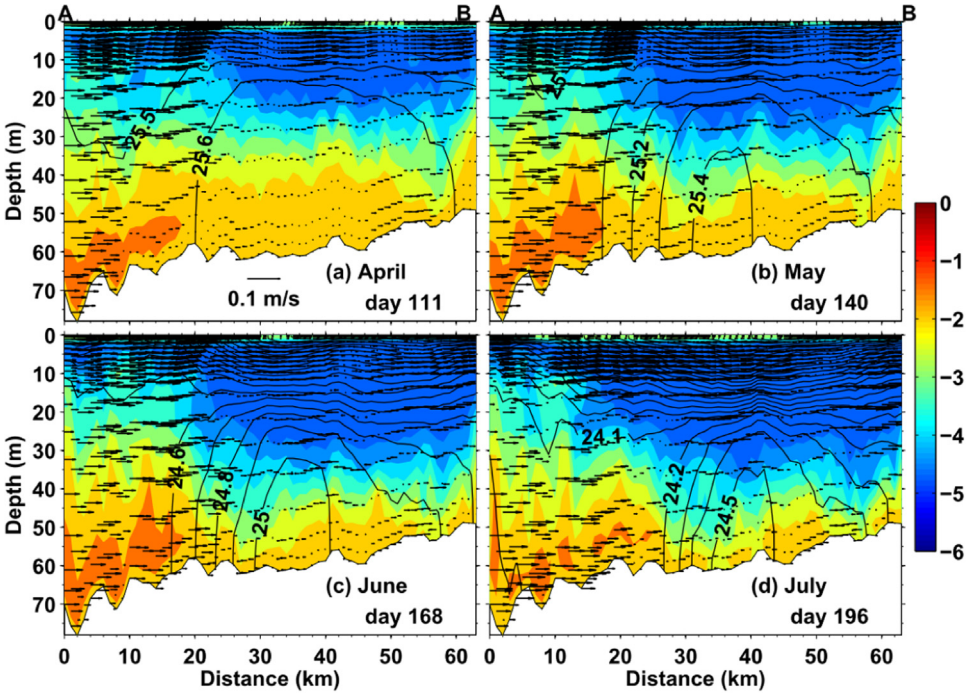

Fig. 16. Vertical distribution of density (kg m^{-3}, black lines), vertical eddy viscosity ($\log_{10}A_z$, m^2 s^{-1}, color), and the current along section AB (m s^{-1}, arrows) in Iyo-nada in (a) April, (b) May, (c) June, and (d) July.

acceleration of temperature increase rate in the BCW of the Iyo-nada.

The accelerating advection of heat by the gradually intensifying gravitational circulation to the BCW in the bottom layer of the Iyo-nada from April to July demonstrates the importance of advection of heat for the large temperature increase in the BCW. The temporal variation of advection of heat also induces variation in the temperature increase rate inside the BCW.

5. Conclusions

In many coastal regions, BCW is usually found in the areas where tidal mixing is relatively weak, such that it cannot transport sufficient heat from sea surface to the bottom water. The temperature increase of BCW from spring to summer has been thought to be due to limited downward heat transport from the thermocline. In some wide regions, such as the North Sea and Yellow Sea, where thermal stratification is in a place over a range of hundreds of kilometers, the temperature increase in the BCW is mainly due to vertical diffusion of heat through the thermocline and thereby, the temperature increase is small (~1 °C) from spring to summer. However, in some relatively smaller regions, such as in the Irish Sea and the nadas in the Seto Inland Sea, where stratification above the BCW is strong, advection from surrounding warm water transports heat to the BCW. Consequently, the temperature increase of the BCW from spring to summer is relatively large (7–10 °C). Moreover, the relative contribution of the advection and vertical diffusion to the change in water temperature differs by region. For example, in the Irish Sea, the advection and vertical diffusion play comparable roles in the warming of the BCW. In contrast, advection contributes as twice of vertical diffusion to the warming of BCW in Iyo-nada in the Seto Inland Sea.

Advection of heat changing with time can produce variation in the temperature increase rate inside the BCW. As demonstrated in the Iyo-nada, advection of heat is associated with gravitational circulation from the Hayasui Strait to the BCW in the bottom layer, which intensifies with increased river discharge and thermal stratification from spring to summer. This makes the temperature increase rate of the BCW accelerate from April to July.

Acknowledgements

This study was supported by the Japanese Ministry of Agriculture, Forestry and Fisheries through the research project 'Development of technologies for mitigation and adaptation to climate change in Agriculture, Forestry and Fisheries' and by grants from the Japanese Ministry of Education, Culture, Sports, Science and Technology (MEXT) to national university corporations for Joint Usage/Research Center. X. Guo is supported by JSPS KAKENHI Grant number JP17H01860. The data used in this paper are available on request to the corresponding author.

References

Blumberg, A.F., Mellor, G.L., 1987. A description of a three dimensional coastal ocean circulation model. Three-Dimensional Coastal Ocean Models, Coastal Estuarine Sci. Monogr 4. Amer. Geophys. Union, pp. 1–16.

Cardona, Y., Bracco, A., 2012. Enhanced vertical mixing within mesoscale eddies due to high frequency winds in the South China Sea. Ocean Modell. 42, 1–15.

Chang, P.-H., Guo, X., Takeoka, H., 2009. A numerical study of the seasonal circulation in the Seto Inland Sea, Japan. J. Oceanogr. 65, 721–736.

Guan, B., 1963. A preliminary study of the temperature variations and the characteristics of the circulation of the cold water mass of the Yellow Sea. Oceanologia Limnol. Sin. 5 (4), 255–284 (in Chinese with English abstract).

Guo, X., Futamura, A., Takeoka, H., 2004. Residual currents in a semi-enclosed bay of the Seto Inland Sea, Japan. J. *Geophys. Res.* 109, C12008. http://dx.doi.org/10.1029/2003JC002203.

Guo, X., Hukuda, H., Miyazawa, Y., Yamagata, T., 2003. A triply nested ocean model for simulating the Kuroshio-roles of horizontal resolution on JEBAR. J. Phys. Oceanogr. 33, 146–169.

Guo, X., Harai, K., Kaneda, A., Takeoka, H., 2013. Simulation of tidal currents and nonlinear tidal interactions in the Seto Inland Sea, Japan. Rep. Res. Inst. Appl. Mech. Kyushu Univ. 145, 43–52.

Hanawa, K., Mitsudera, H., 1985. On daily average of oceanographic data (in Japanese). *Coastal Oceanogr. Bull.* 23, 79–87.

He, C., Wang, Y., Lei, Z., Xu, S., 1959. Preliminary study of the formation of Yellow Sea cold water mass and its property. Oceanologia Limnol. Sin. 2 (1), 11–15 (in Chinese with English abstract).

Holt, J.T., Proctor, R., 2003. The role of advection in determining the temperature structure of the Irish Sea. J. Phys. Oceanogr. 33, 2288–2306.

Horsburgh, K.J., Hill, A.E., 2003. A three-dimensional model of the density- driven circulation in the Irish Sea. J. *Phys. Oceanogr.* 33, 343–365.

James, I.D., 1989. A three-dimensional model of circulation in a frontal region of the North Sea. Deutsche Hydrogr. Zeit. 42, 231–247.

Komorita, T., Guo, X., Fujii, N., Yoshie, N., Takeoka, H., 2016. Nutrient supply from a strait to a coastal basin indicated by the tidal frontal region in the Seto Inland Sea, Japan. Cont. Shelf Res. 112, 68–77. http://dx.doi.org/10.1016/j.csr.2015.10.015.

Lee, T., Liu, W.T., 2005. Effects of high-frequency wind sampling on simulated mixed layer depth and upper ocean temperature. J. Geophys. Res. 110, C05002. http://dx.doi.org/10.1029/2004JC002746.

Liu, Z., Wei, H., Lozovatsky, I.D., Fernando, H.J.S., 2009. Late summer stratification, internal waves, and turbulence in the Yellow Sea. J. Mar. Res. 77, 459–472.

Luyten, P.J., Jones, J.E., Proctor, R., 2003. A numerical study of the long- and short-term temperature variability and thermal circulation in the North Sea. J. Phys. Oceanogr. 33, 37–56.

Mellor, G.L., 2003. Users guide for a three-dimensional, primitive equation, numerical ocean model (2003 version). Atmospheric and Oceanic Sciences Program. Princeton University Rep., pp. 53.

Moon, J.-H., Hirose, N., Yoon, J.-H., 2009. Comparison of wind and tidal contributions to seasonal circulation of the Yellow Sea. J. Geophys. Res. 114, C08016. http://dx.doi.org/10.1029/2009JC005314.

Rippeth, T.P., Wiles, P., Palmer, M.R., Sharples, J., Tweddle, J., 2009. The diapcynal nutrient flux and shear-induced diapcynal mixing in the seasonally stratified western Irish Sea. Cont. Shelf Res. 29, 1580–1587.

Sharples, J., Tett, P., 1994. Modeling the effect of physical variability on the midwater chlorophyll maximum. J. Mar. Res. 52, 219–238.

Simpson, J.H., Hunter, J.R., 1974. Fronts in the Irish Sea. Nature 250, 404–406.

Takeoka, H., Matsuda, O., Yamamoto, T., 1993. Processes causing the Chlorophyll $_{\alpha}$Maximum in the tidal front in Iyo-nada, Japan. J. Oceanogr. 49, 57–70.

Takeoka, H., Ohno, Y., Inahata, N., 1991. Roles of horizontal processes in the formation of density stratification in Hiuchi-nada. J. Oceanogr. Soc. Jpn. 47, 33–44.

Takeoka, H., 2002. Progress in Seto Inland Sea research. J. Oceanogr. 58, 93–107.

Wang, B., Hirose, N., Kang, B., Takayama, K., 2014. Seasonal migration of the Yellow Sea bottom cold water. J. Geophys. Res. Oceans 119, 4430–4443. http://dx.doi.org/10.1002/2014JC009873.

Wang, Q., Guo, X., Takeoka, H., 2008. Seasonal variations of the Yellow River plume in the Bohai Sea: a model study. J. Geophys. Res. 113, C08046. http://dx.doi.org/10.1029/2007JC004555.

Warrach, K., 1998. Modelling the thermal stratification in the North Sea. J. Mar. Syst. 14, 151–165.

Wei, H., Shi, J., Lu, Y.Y., Peng, Y., 2010. Interannual and long-term hydrographic changes in the Yellow Sea during 1977–1998. Deep Sea Res. II 57, 1025–1034.

Wong, K.C., 1994. On the nature of transverse variability in a coastal plain estuary. J. Geophys. Res. 99, 209–222.

Xia, C., Qiao, F., Yang, Y., Ma, J., Yuan, Y., 2006. Three-dimensional structure of the summertime circulation in the Yellow Sea from a wave-tide-circulation coupled model (C11S03). J. Geophys. Res. 111. http://dx.doi.org/10.1029/2005JC003218.

Yanagi, T., Higuchi, H., 1981. Tide and tidal current in the Seto Inland Sea (in Japanese). In: Proc. 28th Conf. on Coastal Engineering,Tokyo, Japan, Japan Society of Civil Engineers, 555–558.

Yu, X., Guo, X., Takeoka, H., 2016. Fortnightly variation in the bottom thermal front and associated circulation in a semi-enclosed sea. J. Phys. Oceanogr. 46, 159–177.

Yu, Y., Gao, H., Shi, J., Guo, X., Liu, G., 2017. Diurnal forcing induces variations in seasonal temperature and its rectification mechanism in the eastern shelf seas of China. J. Geophys. Res. Oceans 122, 9870–9888. http://dx.doi.org/10.1002/2017JC013473.

Yuan, Y.-L., Li, H.-Q., 1993. On the circulation structure and formation mechanism of the cold water mass of the Yellow Sea (I)-Zero-order solution and circulation structure. Sci. China Chem. 36, 1518–1528.

Zhang, S.W., Wang, Q.Y., Lu, Y., Cui, H., Yuan, Y.L., 2008. Observation of the seasonal evolution of the Yellow Sea cold water mass in 1996–1998. Cont. Shelf Res. 28, 442–457.